

Competing failure mechanisms of thin metal films on polymer substrates under tension

Teng Li,^{1,2, a)} Zhao Zhang,¹ and Benoit Michaux¹

¹⁾Department of Mechanical Engineering, University of Maryland, College Park, MD 20742

²⁾Maryland NanoCenter, University of Maryland, College Park, MD 20742

(Received 02 March 2011; accepted 14 May 2011; published online 10 July 2011)

Abstract The ductility of thin metal films on polymer substrates reported in recent experiments has a huge disparity, ranging from less than 1 % up to more than 50 %. To reveal the underpinning origins for such a large variation, this paper reports a systematic computational study of two competing failure mechanisms: metal film necking and grain boundary cracking. The quantitative results suggest that strong grain boundaries and metal/polymer interfacial adhesion are keys to achieve high ductility of polymer-supported metal films. © 2011 The Chinese Society of Theoretical and Applied Mechanics. [doi:10.1063/2.1104102]

Keywords ductility, thin metal films, polymers, nanocrystalline materials, grain boundaries

Rising interests in flexible electronics in recent years have been motivated by the promising future of its potential applications including paper-like displays, printable thin-film solar cells, and skin-like smart prostheses.^{1–3} Such flexible devices will undergo large and repeated stretches, bends and twists during service, therefore require large deformability of device components (e.g., metal interconnects). Thin metal films deposited on polymer substrates are widely used as interconnections and electrodes in flexible devices. Interestingly, the reported failure strains of these polymer-supported thin metal films under tension have a huge disparity, ranging from less than 1 % up to more than 50 %.^{4–14} Such a huge disparity has been accounted for various mechanisms (e.g., metal film necking, film/substrate debonding, and grain boundary cracking) and parameters (substrate stiffness, film thickness, metal grain size, etc.).^{9,14–20} So far, the studies into the effects of these mechanisms and parameters on the large variation of the metal films ductility are suggestive, but not yet systematic. In particular, while the ductility of a polymer-supported metal film is often governed by various competing failure mechanisms, the interplay among these failure mechanisms is far from well understood. To address such an issue, this paper reports a systematic computational study on three major failure mechanisms of thin metal films on polymer substrates (i.e., metal film necking, grain boundary cracking and interfacial debonding), with particular effort on deciphering their competing nature.

Recent experiments and modeling have shed light on the origins of the large variation in the ductility of thin metal films on polymer substrates. Computational modeling predicts that the film/substrate interfacial adhesion plays a crucial role in determining the ductility of polymer supported thin metal films.^{18,20} Under a modest tension, a weakly-adhered metal film can debond from the substrate; the film becomes free-

standing and is free to form a neck, resulting in low ductility. By contrast, a metal film well adherent to a polymer substrate should sustain strains exceeding 80 %. Such a prediction has recently been verified by the tensile tests of thin Cu films on polyimide substrates, in which Cu films well bonded to polyimide substrates can sustain tensile strain above 50 % without fracture, while those poorly bonded to polyimide substrates fracture at strains about 2 %.^{8,10} Both simulations and experiments confirm the co-evolution of metal film necking and film/substrate interfacial debonding when the film/substrate laminate is under tension.^{10,12,18} Furthermore, deformation-associated grain growth in the metal films^{12,21} has been shown to facilitate the metal film necking. Recent experiments also reveal mixed failure mechanisms of both ductile necking and brittle inter-granular cracking in thin metal films on polymer substrates under tension (Fig. 1).⁸ Further simulations on the inter-granular cracking of thin metal films on polymer substrates showed that the rupture strain is also modulated by the grain boundary adhesion and the grain size of the thin metal films.¹⁹

In general, three types of failure mechanisms are observed in tensile tests of a polymer-supported thin metal film: metal film necking, cracking along metal grain boundaries, and film/substrate interfacial debonding. Necking of the thin metal film mainly results from plastic deformation, thus is volume-conserved. In other words, thinning of the metal film leads to an elongation in the tensile direction. By contrast, grain boundary cracking in the metal film involves breaking an array of atomic bonds along the grain boundary, thus only leads to negligible elongation of the metal film. In this sense, the ductile metal film necking is beneficial while the brittle grain boundary cracking is detrimental for achieving high ductility of the metal film. These two competing failure mechanisms can in turn be further modulated by film/substrate interfacial debonding. For example, the debonded part of the metal film becomes freestanding and is more susceptible to necking or grain boundary cracking, resulting in lower ductility.

^{a)}Corresponding author. Email: LiT@umd.edu.

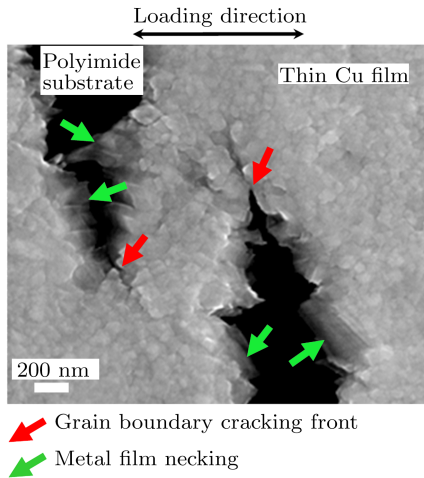


Fig. 1. Scanning electron microscopy image of two neighboring microcracks in an initially continuous thin Cu film (170 nm thick) on a polyimide substrate (125 μm thick) when stretched to 30 %. The microcracks form by a mixture of two competing failure mechanisms: metal film necking and grain boundary cracking. (After Fig. 4(c) in Ref. 8).

Experiments suggest that the fracture of polymer-supported thin metal films is governed by the interplay among these competing failure mechanisms⁸ (e.g., Fig. 1), with quantitative correlation remaining elusive. Existing modeling studies, however, consider these competing failure mechanisms separately, by assuming either perfect grain boundary adhesion or perfect interfacial adhesion.^{18,19} It is desirable to conduct systematic studies to explore the interplay between these competing failure mechanisms from which the parameters underpinning the ductility of polymer-supported thin metal films can be quantitatively determined. We report systematic finite element simulations of the tensile behaviors of thin metal films on polymer substrates in which various combinations of grain boundary adhesion and interfacial adhesion are explored.

Figure 2(a) depicts the simulation model. For simplification, we consider an idealized case of a polymer-supported thin blanket metal film of only one grain along its thickness direction (e.g., a very thin metal film with columnar grains) subjected to uniaxial tension. All grains in the metal film are assumed to have the same size along the tensile direction; the intergranular cracking occurs along grain boundaries perpendicular to the tensile direction (all other grain boundaries are not subjected to cracking, thus are not considered in the simulations). The metal/polymer laminate is taken to deform under the plain strain conditions. Taking advantage of symmetry we model only a unit cell of the laminate, consisting of two halves of adjacent grains, the grain boundary in-between and the substrate underneath (Fig. 2(a)). In the simulation model, the film is a layer of thickness h , and the substrate is a block of thickness $100h$ and length $d = 40h$. The horizontal displacement is set to be zero along the centerline

of the laminate, and set to be $u/2$ along both sides of the laminate. The quantity u/d defines the applied strain. To initiate non-uniform deformation of the metal film, two V-shaped notches, $0.2h$ wide and $0.02h$ deep, are placed at the centers of the top surface of the two neighboring grains (i.e., two top corners in Fig. 2(a)) to introduce imperfection. Both the metal grains and the polymer are modeled as elastic-plastic solids. Under uniaxial tension, the true stress σ and the natural strain ε follow the relation: $\sigma = E\varepsilon$ if $\varepsilon \leq \sigma_Y/E$; $\sigma = \sigma_Y(E\varepsilon/\sigma_Y)^N$ if $\varepsilon > \sigma_Y/E$, where E is Young's modulus, N the hardening exponent, and σ_Y the yield strength. In the simulations, the following values are used: $E = 100$ GPa, $N = 0.02$, and $\sigma_Y = 100$ MPa for the metal; and $E = 8$ GPa, $N = 0.5$ and $\sigma_Y = 50$ MPa for the polymer. These values are representative for Cu films and polyimide substrates, respectively.

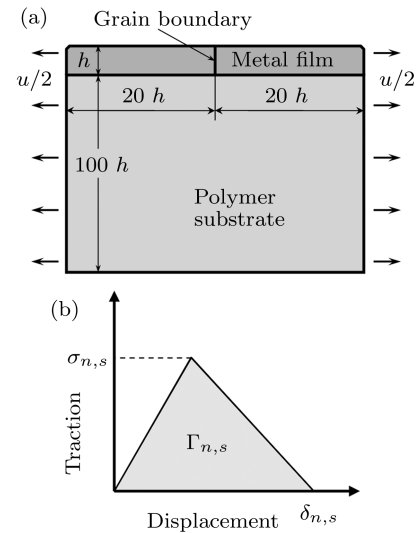


Fig. 2. (a) Schematic diagram of the simulation model: a unit cell of a blanket thin metal film on a polymer substrate, subjected to tension; (b) The traction-separation laws used to model the grain boundary and the metal/polymer interface.

Both the grain boundary and the metal/polymer interface are modeled as an array of nonlinear springs, each of which is characterized by a tensile and a shear traction-displacement law, with six parameters: interfacial tensile strength σ_n and shear strength σ_s , critical opening displacement δ_n and sliding displacement δ_s , and the areas under the traction-displacement curves Γ_n and Γ_s (i.e., the normal and shear adhesion energy of the grain boundary, respectively), as illustrated in Fig. 2(b). We assume that $\sigma_n = \sigma_s$, $\delta_n = \delta_s$, and $\Gamma_n = \Gamma_s$ for both the grain boundary and the metal/polymer interface. In the rest of the paper, we will use $\sigma_{n,s}^{\text{GB}}$, $\delta_{n,s}^{\text{GB}}$, and $\Gamma_{n,s}^{\text{GB}}$ to denote the parameters of the traction-displacement law for the grain boundary, and $\sigma_{n,s}^{\text{INT}}$, $\delta_{n,s}^{\text{INT}}$, and $\Gamma_{n,s}^{\text{INT}}$ for the metal/polymer interface. The grain boundary and the metal/polymer interface are meshed with four-node cohesive elements sharing nodes with the neighboring

Table 1. Interfacial adhesion parameters used in simulations

Interfacial adhesion	$\sigma_{n,s}^{\text{INT}}/\text{MPa}$	$\sigma_{n,s}^{\text{GB}}/\delta_{n,s}^{\text{GB}}/(\text{MPa}\cdot\text{nm}^{-1})$	$\Gamma_{n,s}^{\text{GB}}/(\text{J}\cdot\text{m}^{-2})$
Weak	1	0.2	0.05
Intermediate	50	150	0.3
Strong	100	200	0.5

elements in the film and the substrate. The simulations are performed using finite element code ABAQUS.

To explore the interplay between the interfacial adhesion and grain boundary adhesion on the ductility of thin metal films, we first assume low grain boundary strength and vary the interfacial adhesion, and then assume high grain boundary strength and vary the interfacial adhesion. In each case, we determine the rupture strain and the dominating failure mode of the thin metal films on polymer substrates.

Table 1 lists the values of $\sigma_{n,s}^{\text{INT}}$, $\sigma_{n,s}^{\text{INT}}/\delta_{n,s}^{\text{INT}}$ (interfacial stiffness), and $\Gamma_{n,s}^{\text{INT}}$ used in the simulation to characterize the weak, intermediate and strong interfacial adhesion, respectively. These values are representative of a metal/polymer interface with various adhesion qualities.

Figure 3 plots the failure strains of the thin metal films on polymer substrates as a function of grain boundary adhesion energy $\Gamma_{n,s}^{\text{GB}}$ for weak, intermediate and strong interfacial adhesion, respectively. Here, $\sigma_{n,s}^{\text{GB}} = 50$ MPa and $\sigma_{n,s}^{\text{GB}}/\delta_{n,s}^{\text{GB}} = 100$ MPa/nm, denote low grain boundary strength. Simulating results show that the thin metal films on polymer substrates rupture by grain boundary cracking. For a given interfacial adhesion quality, the failure strain increases as the grain boundary adhesion energy increases, in a roughly linear manner. For a given grain boundary adhesion energy $\Gamma_{n,s}^{\text{GB}}$, the stronger the interfacial adhesion is, the higher the failure strain is. Overall, when the grain boundary strength is low, the failure strain ranges from low to modest. As depicted in the insets in Fig. 3, when the interfacial adhesion is strong, the thin metal film ruptures by grain boundary cracking while the metal/polymer interface remains bonded even though the stress level in the polymer near the grain boundary crack tip is rather high. The constraint from the substrate allows the thin metal film to deform uniformly to a relatively large strain until the grain boundary crack eventually opens up and ruptures the metal film. When the interfacial adhesion is intermediate, the high stress concentration at the interface near the grain boundary causes local debonding. The locally debonded thin metal film facilitates the grain boundary crack opening, leading to a relatively low rupture strain. When the interfacial adhesion is weak, the interfacial debonding occurs at small tensile strain and can easily propagate through the whole interface, leaving the thin metal film nearly freestanding. The lack of substrate constraint results in a rather low rupture strain of the thin metal film due

to grain boundary cracking.

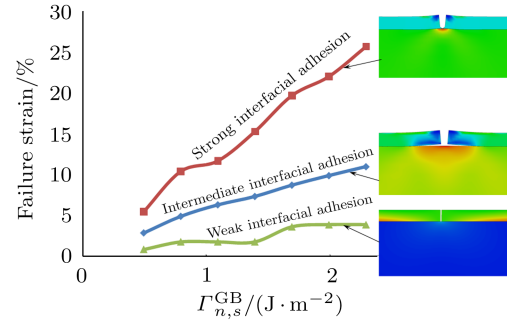


Fig. 3. Failure strain vs. $\Gamma_{n,s}^{\text{GB}}$ grain boundary adhesion energy for various interfacial adhesion qualities. Here grain boundary strength is low ($\sigma_{n,s}^{\text{GB}} = 50$ MPa). Insets show the close-up of grain boundary cracking. Color shades denote von Mises stress. Only partial simulation model is shown.

Figure 4 plots the failure strains of the thin metal film on polymer substrates as a function of $\Gamma_{n,s}^{\text{GB}}$ for weak, intermediate and strong interfacial adhesion, respectively. Here, $\sigma_{n,s}^{\text{GB}} = 150$ MPa and $\sigma_{n,s}^{\text{GB}}/\delta_{n,s}^{\text{GB}} = 100$ MPa/nm denote high grain boundary strength. Simulation results show that the thin metal films on polymer substrates rupture by film necking. As shown in Fig. 4, for a given interfacial adhesion quality, the failure strain is independent of grain boundary adhesion energy. For a given grain boundary adhesion energy $\Gamma_{n,s}^{\text{GB}}$, the stronger the interfacial adhesion, the higher the failure strain. Overall, when the grain boundary strength is high, the failure strain ranges from modest to ultra-high. As depicted in the insets in Fig. 4, when the interfacial adhesion is strong, the thin metal film can deform uniformly to a very large strain (e.g., 100 %) without rupture due to the strong constraint from the polymer substrate. When the interfacial adhesion is intermediate, multiple necks appear in the thin metal film before it eventually ruptures. Each neck (i.e., local thinning) results in a local elongation, adding up to an intermediate rupture strain. When the interfacial adhesion is weak, the interfacial debonding occurs at small tensile strain and can easily propagate through the whole interface, leaving the thin metal film nearly freestanding. The freestanding thin metal film ruptures by forming a single neck near the imperfection location in each grain, leading to a rather low rupture strain. These results agree with those from earlier modeling and experimental studies.^{8,10,18}

In summary, we study two competing failure mechanisms (metal film necking vs. grain boundary cracking) of thin metal films on polymer substrates, through comprehensive computational modeling. We show that, when the grain boundaries of the metal films are weak, the thin metal films tend to rupture by grain boundary cracking. The metal film ductility is modulated by the metal/polymer interfacial adhesion, but in general ranges from low to modest. When the grain boundaries of the metal films are strong, the thin metal films

mainly rupture by necking. There are large variations of the ductility, depending on the interfacial adhesion quality. The above results (e.g., Figs. 3 and 4) are shown to be robust within the range of parameters used in the traction-displacement laws in this paper. While further investigation is necessary on the co-evolution of metal film necking and grain boundary cracking as observed in experiments, the quantitative results from this study suggest that, to achieve high ductility of thin metal films on polymer substrates, it is desirable to have strong grain boundaries of the metal films and strong metal/polymer interfacial adhesion. We therefore call for further experimental verification of the modeling results reported here.

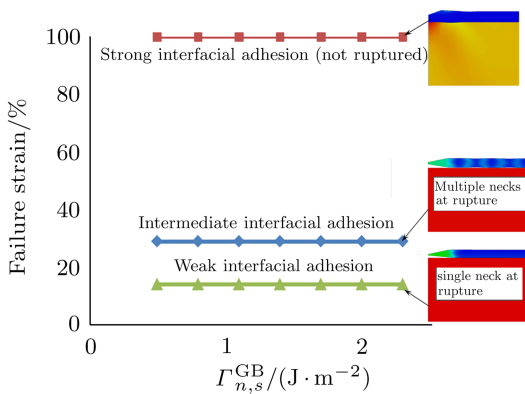


Fig. 4. Failure strain vs. $\Gamma_{n,s}^{GB}$ for various interfacial adhesion qualities. Here grain boundary strength is high ($\sigma_{n,s}^{GB} = 150$ MPa). Insets show the close-up of thin metal film necking. Color shades denote von Mises stress. Only partial simulation model (upper left corner of Fig. 2(a)) is shown.

This work was supported by the Ralph E. Powe Jr. Faculty Award from Oak Ridge Associated Universities, Minta-Martin Foundation and US National Science Foundation (0856540, 0928278), and A. J. Clark Fellowship and UMD Clark School Future Faculty Program

1. G. P. Crawford, *Flexible flat panel displays*, 1st ed., (John Wiley & Sons, Chichester, Hoboken, NJ, 2005).
2. C. J. Brabec, *Solar Cells* **83**, 273 (2004).
3. S. Wagner, S. Lacour, J. Jones, P. Hsu, J. Sturm, T. Li, and Z. Suo, *Physica E - Low-Dimensional Sys. Nanostruct.* **25**, 326 (2004).
4. S. L. Chiu, J. Leu, and P. S. Ho, *J. Appl. Phys.* **76**, 5136 (1994).
5. M. Hommel, and O. Kraft, *Acta Mater.* **49**, 3935 (2001).
6. B. E. Alaca, M. T. A. Saif, and H. Sehitoglu, *Acta Mater.* **50**, 1197 (2002).
7. D. Y. W. Yu, and F. Spaepen, *J. Appl. Phys.* **95**, 2991 (2004).
8. Y. Xiang, T. Li, Z. Suo, and J. Vlassak, *Appl. Phys. Lett.* **87**, 161910 (2005).
9. R. M. Niu, G. Liu, C. Wang, G. Zhang, X. D. Ding, and J. Sun, *Appl. Phys. Lett.* **90**, 161907 (2007).
10. N. S. Lu, X. Wang, Z. G. Suo, and J. Vlassak, *Appl. Phys. Lett.* **91**, 221909 (2007).
11. P. Varguez, F. Aviles, and A. L. Oliva, *Surface Coat. Tech.* **202**, 1556 (2008).
12. N. Lu, X. Wang, Z. Suo, and J. Vlassak, *J. Mater. Res.* **24**, 379 (2009).
13. J. Lohmiller, N. C. Woo, and R. Spolenak, *Mater. Sci. Eng. A-Struct. Mater. Properties Microstruct. Processing* **527**, 7731 (2010).
14. N. S. Lu, Z. Suo, and J. J. Vlassak, *Acta Mater.* **58**, 1679 (2010).
15. T. Li, Z. Huang, Z. Suo, S. Lacour, and S. Wagner, *Appl. Phys. Lett.* **85**, 3435 (2004).
16. T. Li, Z. Huang, Z. Xi, S. Lacour, S. Wagner, and Z. Suo, *Mech. Mater.* **37**, 261 (2005).
17. T. Li, and Z. Suo, *Int. J. Solids Struct.* **43**, 2351 (2006).
18. T. Li, and Z. Suo, *Int. J. Solids Struct.* **44**, 1696 (2007).
19. Z. Zhang, and T. Li, *Scripta Mater.* **59**, 862 (2008).
20. W. Xu, T. J. Lu, and F. Wang, *Int. J. Solids Struct.* **47**, 1830 (2010).
21. T. J. Rupert, D. S. Gianola, Y. Gan, and K. J. Hemker, *Science* **326**, 1686 (2009).